SEMARAK ILMU PUBLISHING

Journal of Advanced Research in Fluid Mechanics and Thermal Sciences

Journal homepage:
https://semarakilmu.com.my/journals/index.php/fluid_mechanics_thermal_sciences/index
ISSN: 2289-7879

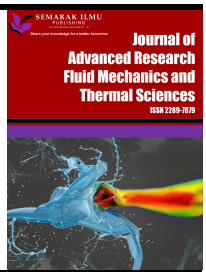

Effect of Sinusoidal Magnetic Field on Peristaltic Flow of Eyring-Powell Nanofluid in an Asymmetric Channel

Asha S. Kotnurkar[1,*], SadafafreenZ. Bagali[1]

[1] Department of Mathematics, Karnatak University Dharwad-580003, Karnataka, India

ARTICLE INFO

Article history:
Received 21 May 2025
Received in revised form 14 January 2026
Accepted 20 March 2026
Available online 23 May 2026

Keywords:
Peristaltic flow; Sinusoidal Magnetic Field; Eyring-Powell nanofluid; Asymmetric Channel

ABSTRACT

This paper aims to investigates the effect of sinusoidal magnetic field on peristaltic flow of Eyring-Powell (E-P) nanofluid in an asymmetric channel. The moment dynamics of the E-P nanofluid, driven by peristalsis and modelled through laws of conservation of concentration, momentum, energy and mass, have been analysed. In the process of mathematical modelling, assumptions such as a small Reynolds number and extended wavelength are employed. By employing the Homotopy Analysis Method (HAM), the solution to the system of coupled non-linear partial differential equations is obtained analytically, contributing to the identification of expressions for temperature, concentration, and velocity. In the result we observe that the Lorentz force act as resisting force, which reduces fluid motion under magnetic field influence. It is also observed that velocity rises with values that are higher of Gr and Qr . This phenomenon occurs because higher thermal Grashof number enhances the buoyancy force due to free convection.The results support developments in physiological applications, industrial fluid transport, and biomedical engineering, including blood flow control and focused drug delivery.

1. Introduction

The concept of peristaltic flow, precisely the peristalsis of E-P nanofluid in an asymmetric channel, has attracted significant interest owing to its important applications in biomedical, industrial, and technical domains. This process is particularly valuable for explaining the progressive wave contractions along a tube or channel. It is notably involved in critical physiological functions such as the swallowing of food through the oesophagus, The ureter moves urine from the kidneys to the urinary bladder, it also moves chyme through the digestive tract, blood moves through small blood vessels, and some organisms, like worms, move around.

Peristaltic pumps are commonly utilized in practical applications, such as roller and finger pumps. For example, in bypass surgery, these devices move slurries and circulate blood in heart-lung machines without coming into contact with the pump's mechanical components. The term "peristaltic" originates from the Greek word Peristaltikos, meaning "clutching" or "compressing." The pioneering work in peristaltic fluid motion was carried out by Latham [1], who first investigated the phenomenon in 1966. Following his research, numerous scientists have explored peristaltic flows in both Newtonian and non-Newtonian fluids [2-4]. Mekheimer [5] examined the movement of a couple of stress fluids in channels that are both smooth and uneven. This mechanism also finds applications in biological and technical domains, including the transport of fluids in various systems and nanofluid technologies. Asha

et. al [6] investigated how surface roughness and induced magnetic field affected the electro-osmosis of E-P nanofluid peristaltic flow in a channel that is not symmetrical. The peristaltic flows of various fluids have been the subject of several investigations, including theoretical [7-8], simulation-based [9-11], and experimental [12–14].

Nanofluids are innovative fluids engineered by dispersing nanoparticles into traditional base fluids such as aqua, hydrocarbon fluid, or ethane-1,2-diol. These nanoparticles are frequently made from materials including metals and their oxides, carbides, or carbon nanotubes, are engineered at the nanometre scale to augment the calorific and physical properties within the fluid. It was Choi [12] who initially introduced the concept, Nanofluids have captured notable attention because of their proficiency for enhancing thermal conductivity, viscosity, and overall efficiency in various applications, such as cooling systems and drug delivery. Chopkar *et. al* [13] examined the impact of particle size on the thermal conductivity of nanofluids. Asha *et. al* [14] studied the impact of heat radiation on a Jeffrey fluid's peristaltic flow with double diffusion while taking gold nanoparticles into account. Nanofluids with magnetic properties have also found applications in fields such as clearing arterial blockages, cancer treatment, and magnetohydrodynamic (MHD) systems. Farooq *et. al* [15] investigated the boundary layer behaviour of magnetic nanofluid flow of second order, enhanced with gyrotactic microbesand carbonnanotubes , for potential applications in medical diagnostics. Despite challenges like low thermal efficiency in devices and environmental concerns due to toxic emissions, ongoing research has highlighted their potential in addressing these issues.

A specialized type of nanofluid is the E-P nanofluid, a non-Newtonian fluid governed by the E-P fluid model. This model, derived from the kinetic theory of liquids, is highly effective in describing the shear-thinning behaviour of substances like human blood, toothpaste, and ketchup. E-P nanofluids have gained attention for their role in peristaltic transport, especially in asymmetric channels, which has important implications in engineering, industrial, and biomedical fields. Noreen S. [16] examined the effect of Magneto-thermo hydrodynamic on peristalsis of E-P nanofluid in an asymmetric channel. The gradual constriction of a wave inside a conduit or tube is characterized by this transport mechanism, offering advanced applications in heat transfer, lubrication, and biological systems. Anum *et. al* [17] conducted an investigation on the combined convective peristaltic movement of E-P nanofluid in a bent channel with complaint wall and Riaz *et. al* [18] explored the impact of hybrid nanoparticles on heat behaviour of peristaltic flow in the E-P fluid model.Mahendra *et. al* [19] investigated bioconvective peristaltic flow of gyrotactic microorganisms in an E-P nanofluid using entropy analysis The findings are highly beneficial when performing particle movements during heart surgery. Research continues to explore their potential, driven by the growing demand for efficient and sustainable technologies [20-21].

The exploration of magnetohydrodynamic (MHD) flow has garnered considerable interest among scholars due to its extensive applications within engineering and industrial contexts.These applications include the creation of cooling systems using liquid metals, as well as in pumps, accelerators, flow sensors, MHD generators, and nuclear power plants. With this in mind, researchers have explored the behaviour of MHD flows across various physical scenarios. Hayat *et. al* [22] investigated impact of magnetic and stretching effects on E-P nanofluid flow over a sheet with changing geometry. Ahmed *et. al* [23] examined analysis of nanofluid flow behaviour in MHD peristaltic motion through porous media with consideration of slip effects. Using damped shear and thermal flux, Qasim *et. al* [24] has studied MHD-induced natural convection of a viscous medium within a vertical cylindricalchannel.Nisar *et.al* [25] analysed the mathematical approach to the Bingham nanofluid's radiative MHD peristalsis.

A sinusoidal magnetic field is a type of magnetic field that exhibits sinusoidal patterns of variation over time and space. The sinusoidal magnetic field is a fundamental concept in

electromagnetism and is used to describe the magnetic fields produced by AC currents, transformers, and inductors. It is also utilized for a wide range of purposes, including MRI (Magnetic Resonance Imagining), wireless power transfer, NMR (Nuclear Magnetic Resonance), and EC (Electromagnetic Compatibility) testing. In addition, sinusoidal magnetic fields are used to study the behaviour of magnetic materials and to develop new magnetic devices and technologies. Overall, the sinusoidal magnetic field is a crucial concept in understanding and working with magnetic fields in a broad spectrum of applications. Suzumura *et. al* [26] studied the behaviours of superconductors under a sinusoidal magnetic field in a 1D configuration.

According to the author, no one has looked into how a sinusoidal magnetic field affects peristaltic flow of E-P nanofluid in an asymmetric channel before. Using the E-P nanofluid, this study intends to examine the effect of a sinusoidal magnetic field on peristaltic flow. The research being conducted has several potential uses in the field of cellular engineering. The research has applications in most medical treatments. The following is how this paper is put together. Using a wave framework, Part 1 builds and refines the mathematical description of the problem, utilizing a small Reynolds number and an extended wavelength.The HAM [27-30] is used to find answers for velocity, temperature, and concentration in Section 2. To obtain series solutions of equations that are linear or not linear, use this general approximate analytics solution. Whether the physical parameters are small or large, this method works for nonlinear problems. Initial approximations and auxiliary linear operators can be chosen with a great deal of flexibility using this method. In order to tackle complex nonlinear problems, it is necessary to convert them into linear subproblems using the right approximations and operators. In the last section, graphs are used to analyse the effects of different physical parameters on concentration,temperature, and velocity.

2. Mathematical Formulation:

Take into account the flow of E-P nanofluid in a 2-dimensional horizontal channel that is $d_1'''+d_2'''$ wide. Along channel walls, sinusoidal waves of length λ move at a constant speed c with time t''', a_1''', a_2''' are waves amplitudes. The Cartesian coordinates X''', Y''' system is set up so that the wave moves across the plane of x. Specifically, the y-axis is taken transversely.The phase difference, denoted by ϕ, varies within the range of $0 \le \phi \le \pi$. It is explained that while the waves are not in phase when $\phi = 0$, the channel is symmetrical, conversely, in the case where $\phi = \pi$, it is the opposite as shown in Fig. 1. Additionally, the factors d_1''', a_1''', d_2''', a_2''', and ϕ must fulfil the following condition, $\left(a_1'''\right)^2+\left(a_2'''\right)^2+2\,a_1'''\,a_2'''\sin\phi \le \left(d_1'''+d_2'''\right)^2$.

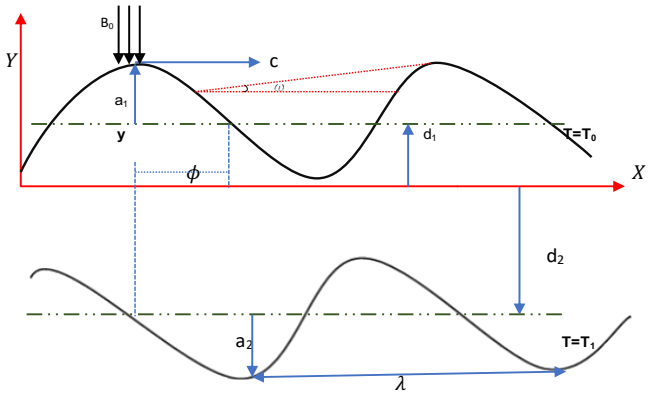

Fig. 1. Diagram of a two-dimensional asymmetric channel

The wall surfaces could be described in terms of its geometry as follows [31]:

$$h_1''' = d_1''' + a_1''' \sin\left[\frac{2\pi}{\lambda}\left(X''' - c\,t'''\right)\right] \quad (1)$$

$$h_2''' = -d_2''' - a_2''' \sin\left[\frac{2\pi}{\lambda}\left(X''' - c\,t'''\right) + \phi\right] \quad (2)$$

The velocity field V [32] is,

$$V = \left[U'''\left(X''', Y''', t'''\right), V'''\left(X''', Y''', t'''\right), 0\right] \quad (3)$$

The study of the E-P fluid model involves the shear of non-Newtonian fluid. The stress tensor of the E-P fluid model is expressed as follows [33-34]:

$$S''' = \mu \nabla V''' + \frac{1}{\beta}\sinh^{-1}\left(\frac{1}{c^*}\nabla V'''\right) \quad (4)$$

where the parameters β and c^* are material constants in the E-P fluid model. μ is the shear viscosity coefficient.

The GE (Governing Equations) for the E-P nanofluid are articulated as outlined:

CE (Continuity Equation) [33]:

$$\frac{\partial U'''}{\partial X'''} + \frac{\partial U'''}{\partial Y'''} = 0 \quad (5)$$

ME (Momentum Equation) [6]:

$$\rho_f\left(\frac{\partial U'''}{\partial t'''}+U'''\frac{\partial U'''}{\partial X'''}+V'''\frac{\partial U'''}{\partial Y'''}\right)=-\frac{\partial P'''}{\partial X'''}+\left(\mu+\frac{1}{\beta C^*}\right)\left(\frac{\partial^2 U'''}{\partial\left(X'''\right)^2}+\frac{\partial^2 U'''}{\partial\left(Y'''\right)^2}\right)$$
$$-\sigma\left(B_0 k\sin 2\pi\omega t'''\right)^2 U'''-\frac{1}{2\beta C^{*3}}\left(\frac{\partial U'''}{\partial X'''}+\frac{\partial U'''}{\partial Y'''}\right)^2\left(\frac{\partial^2 U'''}{\partial\left(X'''\right)^2}+\frac{\partial^2 U'''}{\left(Y'''\right)^2}\right) \quad (6)$$
$$+\rho_f g\kappa\left(T'''-T_0\right)+\rho_f g\kappa\left(C'''-C_0\right)$$

$$\rho_f\left(\frac{\partial V'''}{\partial t'''}+U'''\frac{\partial V'''}{\partial X'''}+V'''\frac{\partial V'''}{\partial Y'''}\right)=-\frac{\partial P'''}{\partial Y'''}+\left(\mu+\frac{1}{\beta C^*}\right)\left(\frac{\partial^2 V'''}{\partial\left(X'''\right)^2}+\frac{\partial^2 V'''}{\partial\left(Y'''\right)^2}\right)$$
$$-\sigma(B_0 k\sin 2\pi\omega t''')^2 V'''-\frac{1}{2\beta C^{*3}}\left(\frac{\partial V'''}{\partial\widetilde{X}}+\frac{\partial V'''}{\partial\widetilde{Y}}\right)^2\left(\frac{\partial^2 V'''}{\partial\widetilde{X}^2}+\frac{\partial^2 V'''}{\partial\widetilde{Y^2}}\right) \quad (7)$$

EE (Energy Equation) [16]:

$$\left(\rho c\right)_f\left(\frac{\partial T'''}{\partial t'''}+U'''\frac{\partial T'''}{\partial X'''}+V'''\frac{\partial T'''}{\partial Y'''}\right)=k^*\left(\frac{\partial^2 T'''}{\partial\left(X'''\right)^2}+\frac{\partial^2 T'''}{\partial\left(Y'''\right)^2}\right)$$
$$+\left(\rho c\right)_p D_B\left(\frac{\partial C'''}{\partial X'''}+\frac{\partial C'''}{\partial Y'''}\right)\left(\frac{\partial T'''}{\partial X'''}+\frac{\partial T'''}{\partial Y'''}\right)+\left(\rho c\right)_p\frac{D_T}{T_m}\left(\frac{\partial^2 T'''}{\partial\left(X'''\right)^2}+\frac{\partial^2 T'''}{\partial\left(Y'''\right)^2}\right)^2 \quad (8)$$

Concentration Equation [14]:

$$\frac{\partial C'''}{\partial t'''}+U'''\frac{\partial C'''}{\partial X'''}+V'''\frac{\partial C'''}{\partial Y'''}=D_B\left(\frac{\partial^2 C'''}{\partial\left(X'''\right)^2}+\frac{\partial^2 C'''}{\partial\left(Y'''\right)^2}\right)+\frac{D_T}{T_m}\left(\frac{\partial^2 T'''}{\partial\left(X'''\right)^2}+\frac{\partial^2 T'''}{\partial\left(Y'''\right)^2}\right) \quad (9)$$

The connection between the WF (Wave Frame) and the laboratory is presented by [35]:

$$\left.\begin{aligned} x'''=X'''-c\,t''', \qquad & y'''=Y''' \\ u'''\left(x''',y'''\right)=U'''-c, \quad & v'''\left(x''',y'''\right)=V''' \end{aligned}\right\} \quad (10)$$

where $\left(x''',\, y'''\right)$ and $\left(u''',v'''\right)$ denote coordinates and component in WF (Wave Frame).

Velocity field is articulated through stream function, where $u=\frac{\partial\psi}{\partial y},\quad v=-\delta\frac{\partial\psi}{\partial x}$.

Relevant boundary conditions for aforementioned problem are provided

$$\left.\begin{aligned}
&\psi''' = \frac{q}{2}, \quad u''' = \frac{\partial \psi'''}{\partial \tilde{y}} = c, \quad C''' = C_0''', \quad T''' = T_0''', \quad Y''' = h_1''' \\
&\psi''' = -\frac{q}{2}, \; u''' = \frac{\partial \psi'''}{\partial \tilde{y}} = -c, \quad C''' = C_0''', \quad T''' = T_0''', \; Y''' = h_1'''
\end{aligned}\right\} \tag{11}$$

Introducing the subsequent dimensionless parameters:

$$\left.\begin{aligned}
&\psi = \frac{\psi'''}{ca}, \; x = \frac{x'''}{\lambda}, \; X = \frac{X'''}{\lambda}, \; y = \frac{y'''}{a}, \; Y = \frac{Y'''}{a}, \; u = \frac{u'''}{c}, \; v = \frac{v'''}{c}, \; t = \frac{c\,t'''}{\lambda}, \; \delta = \frac{a}{\lambda}, \\
&p = \frac{a^2 p'''}{c\lambda\mu}, \mathrm{Re} = \frac{2\rho_f ca}{\mu}, \; A = \frac{Bc^2}{2a^2 c^{*^2}}, \; B = \frac{1}{\mu\beta c^*}, \; F = \frac{q}{ca}, \; M = \sqrt{\frac{\sigma}{\mu}} B_0 a, \; \omega = \frac{c}{\lambda} \\
&\Omega = \frac{C''' - C_0'''}{C_1''' - C_0'''}, \; \theta = \frac{T''' - T_0'''}{T_1''' - T_0'''}, \; Gr = \frac{\rho_f g k a^2 \left(T_1''' - T_0'''\right)}{c\mu}, \; Qr = \frac{\rho_f g k a^2 \left(C_1''' - C_0'''\right)}{c\mu}, \\
&\beta^* = \frac{k^*}{(\rho c)_f}, \; \mathrm{Pr} = \frac{\mu}{\beta^*}, \; Nb = \frac{(\rho c)_p D_B \left(C_1''' - C_0'''\right)}{(\rho c)_f \mu}, \; Nt = \frac{(\rho c)_p D_T \left(T_1''' - T'''\right)}{(\rho c)_f T_m \mu},
\end{aligned}\right\} \tag{12}$$

The following are the dimensionless symbols for the quantities discussed earlier: ψ is stream function, μ is dynamic viscosity, p is non dimensional pressure, F is non dimensional average flux in WF (Wave Frame), $(A \; and \; B)$ are the dimensionless E-P nanofluid parameters, (M) is Hartmann Number , (LTGN) Local Temperature Grashof Number (Gr) and (LNMTGN) Local Nanoparticle Mass Transfer Grashof Number (Qr), θ is temperature distribution, Ω is mass concentration, Pr is PN (Prandtl Number), Nt is TP (Thermophoresis Parameter), Nb is BMP (Brownian Motion Parameter).

The momentum equation simplifies as its nonlinear terms vanish; assumptions such as a small Reynolds number and extended wavelength are employed, where $\mathrm{Re} = \frac{2\rho_f ca}{\mu}$ denotes the Renolds number, and δ signifies the wave number. Velocity fields are characterized by stream functions $u = \frac{\partial \psi}{\partial y}, \quad v = -\delta \frac{\partial \psi}{\partial x}$, the equations are

$$\frac{\partial p}{\partial x} = (1+B)\frac{\partial^3 \psi}{\partial y^3} - A\left(\frac{\partial^2 \psi}{\partial y^2}\right)^2 \frac{\partial^3 \psi}{\partial y^3} - M^2 (k \sin 2\pi\omega t)\frac{\partial \psi}{\partial y} + Gr\theta + Qr\Omega, \tag{13}$$

$$(1+B)\frac{\partial^4 \psi}{\partial y^4} - A\left(\left(\frac{\partial^2 \psi}{\partial y^2}\right)^2 \frac{\partial^4 \psi}{\partial y^4} + 2\left(\frac{\partial^3 \psi}{\partial y^3}\right)^2 \frac{\partial^2 \psi}{\partial y^2}\right) - M^2 (k \sin 2\pi\omega t)\frac{\partial^2 \psi}{\partial y^2} + Gr\frac{\partial \theta}{\partial y} + Qr\frac{\partial \Omega}{\partial y} = 0, \tag{14}$$

$$\frac{\partial p}{\partial y} = 0, \tag{15}$$

$$\frac{\partial^2\theta}{\partial y^2}+\Pr Nb\frac{\partial\theta}{\partial y}\frac{\partial\Omega}{\partial y}+\Pr Nt\left(\frac{\partial\theta}{\partial y}\right)^2=0, \tag{16}$$

$$\frac{\partial^2\Omega}{\partial y^2}+\frac{Nt}{Nb}\frac{\partial^2\theta}{\partial y^2}=0, \tag{17}$$

The boundary conditions without dimensions can be formulated in the following manner:

$$\left.\begin{aligned}&\psi=\frac{F}{2},\quad \Omega=0,\ \theta=0,\ \frac{\partial\psi}{\partial y}=-1\quad at\quad Y=h_1''',\\&\psi=-\frac{F}{2},\ \Omega=1,\quad \theta=1,\quad \frac{\partial\psi}{\partial y}=-1\quad at\quad Y=h_2'''.\end{aligned}\right\} \tag{18}$$

where independent of dimension mean flow rate over time F in WF (Wave Frame) can be correlated with that in the laboratory frame through the following equation:

$$\Theta=F+1,\qquad F=\int_{h_1}^{h_2}\frac{\partial\psi}{\partial y}dy, \tag{19}$$

The rate of volume flow is

$$Q=\int_{h2}^{h1}(u+1)\,dy \tag{20}$$

3. Method of Solution

By means of analysis of equations (14)-(17) and related boundary conditions (18), the solution is found to be an even function of (14)-(17). In addition to observing that equations (14)-(17) include term y, it's advantageous to represent (17) as $\Omega(y)$,(16) as $\theta(y)$ and (14) as $u(y)$ via polynomials of power. In the HAM, we determine auxiliary linear operators and compute the initial guesses in the following form:

$$\psi_0(y)=-\left(1-\frac{F}{h_2-h_1}\right)\left(\begin{aligned}&\frac{2}{(h_2-h_1)^2}y^3-\frac{3(h_1+h_2)}{(h_2-h_1)^2}y^2+\left(\frac{F}{h_2-h_1-F}+\frac{(h_1+h_2)^2+2h_1h_2}{(h_2-h_1)^2}\right)y\\&-\left(\frac{F(h_2-h_1)}{2(h_2-h_1-F)}+\frac{h_1h_2(h_1+h_2)}{(h_1-h_2)^2}+\frac{h_1F}{(h_2-h_1-F)}\right)\end{aligned}\right) \tag{21}$$

$$\theta_0(y)=\frac{h_1-y}{h_1-h_2}, \tag{22}$$

$$\Omega_0(y)=\frac{h_1-y}{h_1-h_2}, \tag{23}$$

The auxiliary linear operators that correspond to equation (14), (16) and (17) are

$$L_\psi = \frac{\partial^6}{\partial y^6},\ L_\theta = \frac{\partial^2}{\partial y^2},\ L_\Omega = \frac{\partial^2}{\partial y^2}, \tag{24}$$

with property

$$\left.\begin{aligned} &L_\psi\left[\zeta_1+\zeta_2 y+\zeta_3\frac{y^2}{2}+\zeta_4\frac{y^3}{3}+\zeta_5\frac{y^4}{4}+\zeta_6\frac{y^5}{6}\right]=0,\\ &L_\theta\left[\zeta_1+\zeta_2 y\right]=0, \qquad L_\Omega\left[\zeta_1+\zeta_2 y\right]=0, \end{aligned}\right\} \tag{25}$$

where $\zeta_1, \zeta_2, \zeta_3, \zeta_4, \zeta_5$ *and* ζ_6 are arbitrary constants, the deformation equations of zeroth-order are

$$(1-\xi)L_\psi\left[\psi(y;\xi)-\psi_0(y)\right]=\xi H_\psi h_\psi N\left[\psi(y;\xi)\right], \tag{26}$$

$$(1-\xi)L_\theta\left[\theta(y;\xi)-\theta_0(y)\right]=\xi H_\theta h_\theta N\left[\theta(y;\xi)\right], \tag{27}$$

$$(1-\xi)L_\Omega\left[\Omega(y;\xi)-\Omega_0(y)\right]=\xi H_\Omega h_\Omega N\left[\Omega(y;\xi)\right], \tag{28}$$

In this context, the embedding parameter is $\xi\in[0,1]$, while the auxiliary parameters are h_ψ, h_θ and h_Ω. Additionally, the auxiliary functions are H_ψ, H_θ and H_Ω, along with the corresponding auxiliary linear and non-linear operators L and N respectively. The unknown functions are $\psi(y;\xi), \theta(y;\xi)$ and $\Omega(y;\xi)$, as well as the initial approximations $\psi_0(y), \theta_0(y)$ and $\Omega_0(y)$ for $\psi(y), \theta(y)$ and $\Omega(y)$ functions.

Using Equations (26)-(28), we can systematically formulate the associated equations along with their respective boundary conditions. By employing theHAM, the obtained solutions are represented as follows:

$$\psi(y,\xi)=\psi_0(y)+h_\psi\psi_1(y)+h_\psi^2\psi_2(y)+h_\psi^3\psi_3(y)+\ldots\ldots\ldots\ldots \tag{29}$$

$$\theta(y,\xi)=\theta_0(y)+h_\theta\theta_1(y)+h_\theta^2\theta_2(y)+h_\theta^3\theta_3(y)+\ldots\ldots\ldots\ldots \tag{30}$$

$$\Omega(y,\xi)=\Omega_0(y)+h_\Omega\Omega_1(y)+h_\Omega^2\Omega_2(y)+h_\Omega^3\Omega_3(y)+\ldots\ldots\ldots\ldots \tag{31}$$

4. Results and Discussion

This paper examines the effect of sinusoidal magnetic field on peristaltic flow of E-P nanofluid in an asymmetric channel. The analytical results for temperature, concentration and velocity are acquired through Mathematica software. The findings are discussed in this section and are visually represented through graphs illustrated with ORIGIN software. The equations are formatted using MathType for clarity and precision.As indicated in Table (1), we have contrasted the obtained results with the numerical findings of Prakshaet *al.,* [36]. It is found to be in good agreement with the results of the present study.

Table (1)
The current analytical solution is compared to the solution by Prakash *et al*. [36] for various values of y when $Q=2,\ A=B=M=k=Gr=Qr=0$

y	Prakasha *et al.*,[36]	Present Work
1	2	2
0.8	2.032	2.043
0.6	1.776	1.794
0.5	1.5625	1.565
0.4	1.304	1.320
0.2	0.668	0.703
0	0	0

4.1 Velocity Distribution:

The implications of E-P nanofluid parameters $(A\ and\ B)$, Hartmann number (M), (LTGN) Local Temperature Grashof Number (Gr) and (LNMTGN) Local Nanoparticle Mass Transfer Grashof Number Qr on the velocity profile (u) are illustrated in Fig. 2(a) to Fig.2(e) It has been noted from Fig. 2(a) and Fig. 2(b) that as the E-P fluid parameter goes up, the velocity u decreases. This occurs because fluid parameters are inversely related to viscosity. Additionally, an enhancement in M results in a diminution of velocity u. It has been pointed out that in fluid flow, the Lorentz force act as resisting force, which results in a reduction of fluid motion when subjected to a magnetic field, as demonstrated in Fig2(c).Fig. 2(d) and Fig.2(e) have been used to show the influence of the Gr and Qr on velocity. It has been observed that velocity rises with values that are higher. of Gr and Qr. This phenomenon occurs because higher thermal Grashof number enhances the buoyancy force due to free convection. Studies of this nature have been found to be useful in medical applications.

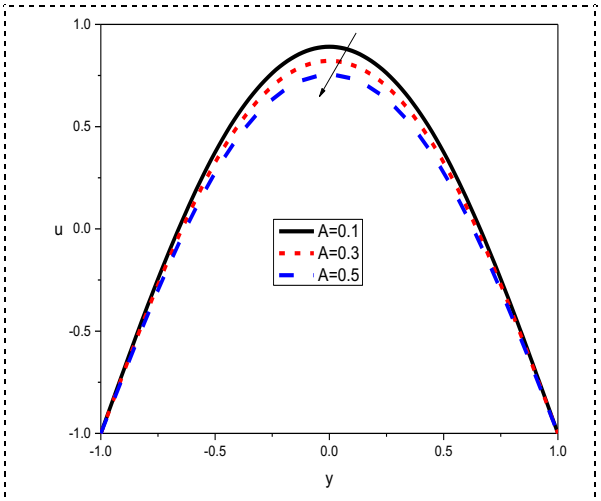

Fig.2(a): Influence of A on the behaviour of u, When $B=1,\ M=2,\ Gr=2\ \ and\ \ Qr=2.$

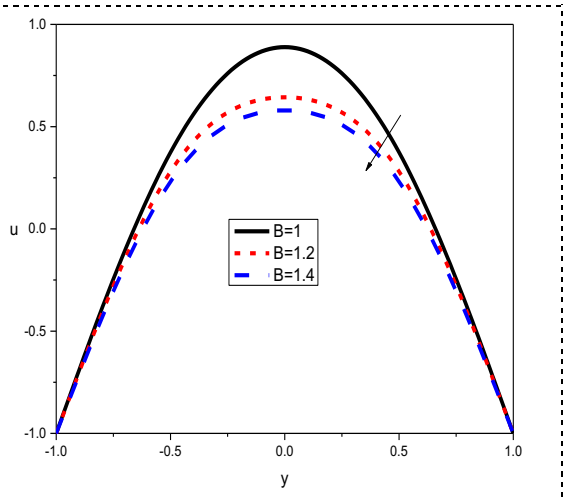

Fig.2(b): Influence of B on the behaviour of u, When $A=0.5,\ M=2\ Gr=2\ \ and\ \ Qr=2.$

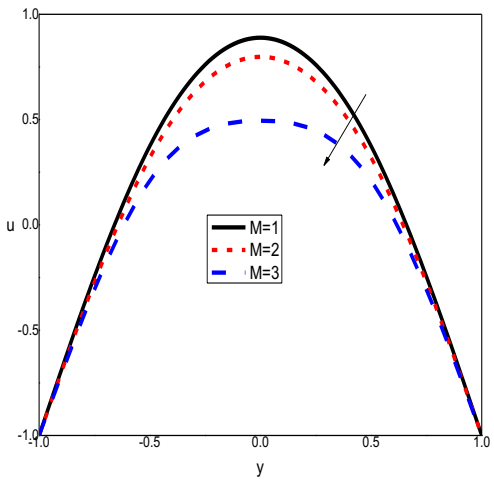

Fig.2(c): Influence of M on the behaviour of u, When $A = 0.5, B = 1, Gr = 2$ *and* $Qr = 2$.

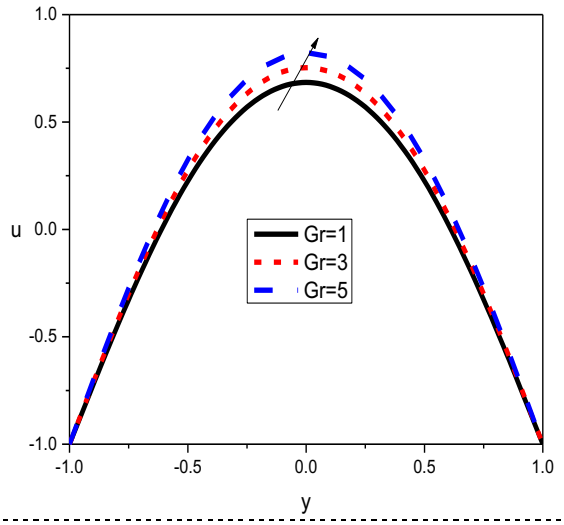

Fig.2(d): Influence of Gr on the behaviour of u, When $A = 0.1, B = 1.2, M = 1,$ *and* $Qr = 2$

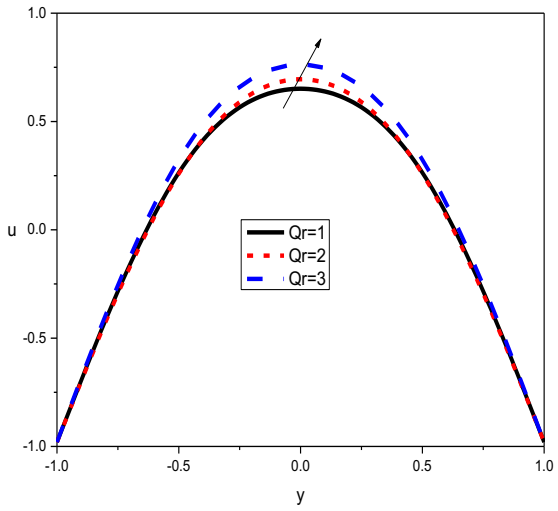

Fig. 2(e): Influence of Qr on the behaviour of u, When $A = 0.1, B = 1.2, M = 1$ *and* $Gr = 3$.

4.2 Temperature Distribution:

Fig.3(a) to Fig.3(c) illustrate how temperature (θ) varies with Nb, Nt and Pr. The results indicate that temperature increases as Nb rises but diminishes with an escalation in Nt and Pr. Since, Nb represents Brownian motion, which governs the moment of fluid particles, it contributes to a rise in temperature. Conversely, the thermophoresis parameter exhibits the opposite effect because thermophoresis involves particle moment from regions of higher temperature to lower temperature due to a thermal gradient. Meanwhile, Pr influences temperature distribution as it represents the ratio of fluid moment to thermal diffusivity. Lower thermal diffusivity results in a higher Pr, ultimately leading to a reduction in temperature.

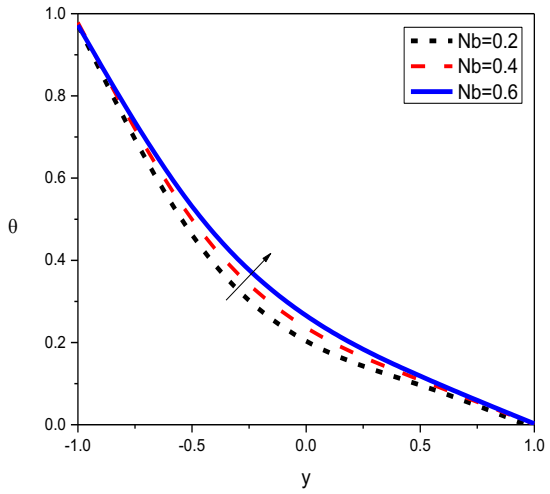

Fig.3(a): Influence of Nb on the behaviour of θ, When $Nt = 0.4 \; and \;\; Pr = 2$.

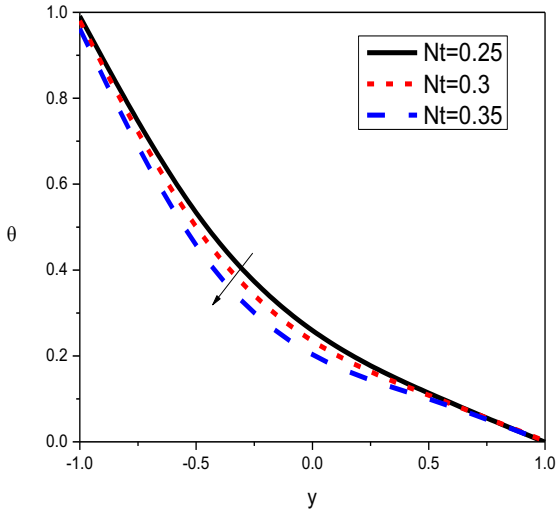

Fig.3(b). Influence of Nt on the behaviour of θ, When $Nb = 0.4 \; and \;\; Pr = 2$.

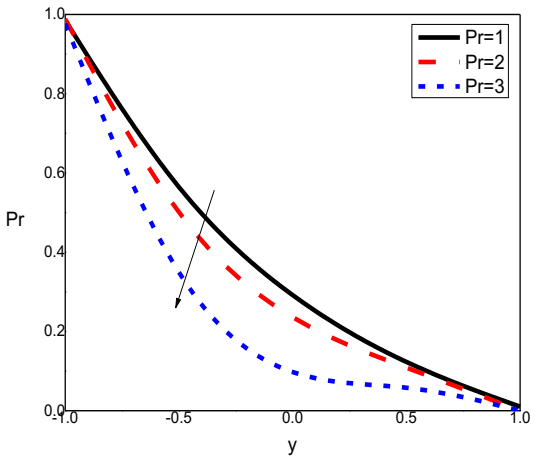

Fig. 3(c): Influence of Pr on the behaviour of θ, When $Nb = 0.4 \; and \;\; Nt = 0.4$.

4.3 Concentration Profile

Fig. 4(a) and Fig.4(b) illustrates the impact of different physical parameters, namely BMP (Brownian Motion Parameter) Nb and TP (Thermophoresis Parameter) Nt on the nanoparticle concentration profile (Ω). In Fig.4(a) it is evident that concentration of nanoparticle rises as Nb increases. This phenomenon occurs due to the substantial moment of nanoparticles from the cooler region to the warmer region, leading to an enhancement in concentration distribution. Fig.4(b) depicts the influence of the TP (Thermophoresis Parameter) Nt. As parameter rises, the concentration of

nanoparticles diminishes. The reduction of nanoparticles concentration is attributed to interference in fluid molecules. In thermophoresis, particles migrate away from the heated region towards the cooler zone, creating disturbances in the nanoparticles moment which is ultimately results in a decrease in their concentration.

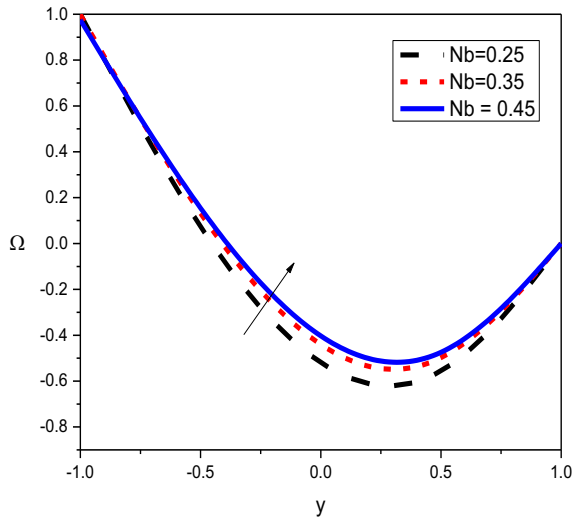

Fig. 4(a): Influence of Nb on the behaviour of Ω, When $Nt = 0.4 \; and \;\; Pr = 3.5$.

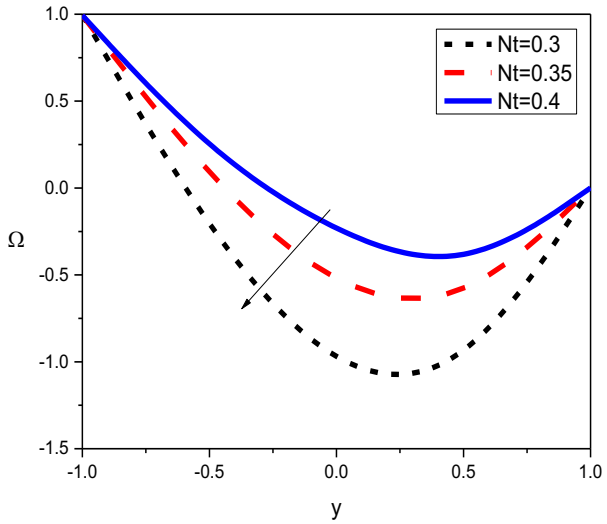

Fig. 4(b): Influence of Nt on the behaviour of Ω, When $Nb = 0.4 \; and \;\; Pr = 3.5$.

5. Conclusions

In this analysis, we researched on the effect of sinusoidal magnetic field on peristaltic flow of E-P nanofluid in an asymmetric channel. The non-dimension non-linear coupled PDE's are solved by HAM. It was examined how emerging parameters affect the governing equations. Based on the analysis, it was concluded that the following outcomes could be derived.

- The E-P fluid parameter $(A \; and \; B)$ goes up, the velocity u decreases. This occurs because fluid parameters are inversely related to viscosity. Additionally, an enhancement in M results in a diminution of velocity u. It has been pointed out that in fluid flow, the Lorentz force act as resisting force, which results in a reduction of fluid motion when subjected to a magnetic field.
- It is observed that velocity rises with values that are higher of Gr and Qr. This phenomenon occurs because higher thermal Grashof number enhances the buoyancy force due to free convection.
- Nb represents Brownian motion, which governs the moment of fluid particles, and contributes to a temperature increase. The thermophoresis parameter Nt, on the other hand, has the opposite effect because it involves particle moment moving from higher to lower temperatures due to a thermal gradient. Meanwhile, temperature distribution $\Pr$ is influenced by the ratio of fluid moment to thermal diffusivity. Lower thermal diffusivity results in a higher, eventually leading to a temperature decrease.
- As the temperature rises, the concentration of Nb nanoparticles grows because they migrate significantly from the cooler to the warmer region, resulting in an improved distribution of concentrations, whereas the effect observed for Nt is the opposite.

6. Nomenclature

(Gr)	Local Temperature Grashof Number
(Qr)	Nanoparticle Mass Transfer Grashof Number
(M)	Hartmann Number
(Pr)	Prandtl Number
$(A\ and\ B)$	Dimensionless E-P nanofluid parameters
Nt	Thermophoresis Parameter
Nb	Brownian Motion Parameter
ϕ	Phase Difference
U''' and V'''	Velocity components
X''' and Y'''	Coordinate Axes
P'''	Pressure
ρ_f	Fluid Density
σ	Fluid Electrical Conductivity
B_0	Applied Magnetic Field
ω	Angular Frequency
t'''	Time Variable
T'''	Fluid Temperature
C'''	Nanoparticle Concentration
D_B	Brownian Diffusion Coefficient
$(\rho_c)_f$	Fluid Heat Capacity
D_T	Thermophoresis Diffusion
k^*	Thermal Conductivity
$(\rho_c)_p$	Effective Heat Capacity of Nanoparticle Material
g	Acceleration due to Gravity
T_m	Fluid Mean Temperature
κ	Volume Expansion Coefficient
k	Non- Dimensional Constant
x	Dimensionless Axial Coordinate
y	Dimensionless Transverse Coordinate

Acknowledgement
Not Applicable

References

[1] Latham, Thomas Walker. "Fluid motions in a peristaltic pump." PhD diss., Massachusetts Institute of Technology, 1966.

[2] Fung,Y. C., and C. S. Yih. "Peristaltic transport."*Journal of Fluid Mechanics* 35, (1968): 669-675. DOI:https://doi.org/10.1115/1.3601290.
[3] Mishra, Manoranjan, and A. Ramachandra Rao. "Peristaltic transport of a Newtonian fluid in an asymmetric channel." *Zeitschrift für angewandte Mathematik und Physik ZAMP* 54 (2003): 532-550.DOI: 10.1007/s00033-003-1070-7.
[4] Dhinakaran, Vedhesh, Keerthi Devarajan Anuradha, J. U. Viharika, Umair Khan, Nermeen Abdullah, and Samia Elattar. "Effectiveness of heat source/sink and Lorentz force constraints in a non-Newtonian peristaltic arterial blood hybrid nanofluid past an overlapping stenotic artery." *Case Studies in Thermal Engineering* 65 (2025): 105577.DOI:https://doi.org/10.1016/j.csite.2024.105577.
[5] Mekheimer, Kh S. "Peristaltic transport of a couple stress fluid in a uniform and non-uniform channels." *Biorheology* 39,no. 6 (2002): 755-765.DOI:https://doi.org/10.1177/0006355X2002039006004.
[6] Kotnurkar, Asha, and Namrata Kallolikar. "Effect of surface roughness and induced magnetic field on electro-osmosis peristaltic flow of Eyring Powell nanofluid in a tapered asymmetric channel." *Journal of Advanced Research in Numerical Heat Transfer* 10 (2022): 20-37. DOI:https://doi.org/10.1007/s10867-022-09603-1.
[7] Nadeem, S., and Iqra Shahzadi. "Mathematical analysis for peristaltic flow of two phase nanofluid in a curved channel." *Communications in Theoretical Physics* 64, no. 5 (2015): 547.DOI: 10.1088/0253-6102/64/5/547.
[8] Yasmeen, Shagufta, Saleem Asghar, Hafiz Junaid Anjum, and Tayyaba Ehsan. "Analysis of Hartmann boundary layer peristaltic flow of Jeffrey fluid: Quantitative and qualitative approaches." *Communications in Nonlinear Science and Numerical Simulation* 76 (2019): 51-65.DOI:https://doi.org/10.1016/j.cnsns.2019.01.007.
[9] Palmada, Nadun, John E. Cater, Leo K. Cheng, and Vinod Suresh. "Experimental and computational studies of peristaltic flow in a duodenal model." *Fluids* 7, no. 1 (2022): 40.DOI:https://doi.org/10.3390/fluids7010040.
[10] Qureshi, Imran Haider, Muhammad Awais, Saeed Ehsan Awan, Muhammad Nasir Abrar, Muhammad Asif Zahoor Raja, Sayer Obaid Alharbi, and I. Khan. "Influence of radially magnetic field properties in a peristaltic flow with internal heat generation: Numerical treatment." *Case Studies in Thermal Engineering* 26 (2021): 101019.DOI:https://doi.org/10.1016/j.csite.2021.101019.
[11] Ashtari, O., M. Pourjafar-Chelikdani, K. Gharali, and K. Sadeghy. "Peristaltic transport of elliptic particles:a numerical study." *Physics of Fluids* 34, no. 2 (2022).DOI:https://doi.org/10.1063/5.0080870.
[12] Choi, S. US, and Jeffrey A. Eastman. *Enhancing thermal conductivity of fluids with nanoparticles*. No. ANL/MSD/CP-84938; CONF-951135-29. Argonne National Lab.(ANL), Argonne, IL (United States), 1995.
[13] Chopkar, M., S. Sudarshan, P. K. Das, and I. Manna. "Effect of particle size on thermal conductivity of nanofluid." *Metallurgical and materials transactions A* 39 (2008): 1535-1542.DOI: 10.1007/s11661-007-9444-7.
[14] Kotnurkar, Asha S., and Sunitha, G. "Influence of thermal radiation on peristaltic blood flow of a Jeffrey fluid with double diffusion in the presence of gold nanoparticles." *Informatics in Medicine Unlocked* 17 (2019): 100272.DOI:https://doi.org/10.1016/j.imu.2019.100272.
[15] Farooq, Umar, Tao Liu, and Ahmed Jan. "Boundary Layer Analysis of Second-Order Magnetic Nanofluid Flow with Carbon Nanotubes and Gyrotactic Microorganisms for Medical Diagnostics." *BioNanoScience* 15, no. 1 (2025): 1-16.DOI: https://doi.org/10.1007/s12668-024-01763-9.
[16] Noreen, Saima. "Magneto-thermo hydrodynamic peristaltic flow of Eyring-Powell nanofluid in asymmetric channel." *Nonlinear Engineering* 7, no. 2 (2018): 83-90.DOI: doi.org/10.1515/nleng-2017-0069.
[17] Tanveer, Anum, Tasawar Hayat, Fuad Alsaadi, and Ahmed Alsaedi. "Mixed convection peristaltic flow of Eyring-Powell nanofluid in a curved channel with compliant walls." *Computers in Biology and Medicine* 82 (2017): 71-79.DOI:https://doi.org/10.1016/j.compbiomed.2017.01.015.
[18] Riaz, Arshad, R. Ellahi, and Sadiq M. Sait. "Role of hybrid nanoparticles in thermal performance of peristaltic flow of Eyring–Powell fluid model." *Journal of Thermal Analysis and Calorimetry* 143 (2021): 1021-1035.DOI:https://doi.org/10.1007/s10973-020-09872-9.
[19] Mahendra, D. L., J. U. Viharika, V. Ramanjini, O. D. Makinde, and U. B. Vishwanatha. "Entropy analysis on the bioconvective peristaltic flow of gyrotactic microbes in Eyring-Powell nanofluid through an asymmetric channel." *Journal of the Indian Chemical Society* 100, no. 3 (2023): 100935. DOI: https://doi.org/10.1016/j.jics.2023.100935.
[20] Anjum, Nazash, W. A. Khan, A. Hobiny, M. Azam, M. Waqas, and M. Irfan. "Numerical analysis for thermal performance of modified Eyring Powell nanofluid flow subject to activation energy and bioconvection dynamic." *Case Studies in Thermal Engineering* 39 (2022): 102427. DOI:https://doi.org/10.1016/j.csite.2022.102427.
[21] Khan, M. Waleed Ahmed, Imad Khan, and Muhammad Asif. "Applications of neural networking in Eyring-Powell nanofluid dynamics on a rotating surface in a porous medium." *Alexandria Engineering Journal* 108 (2024): 568-582.DOI:https://doi.org/10.1016/j.aej.2024.07.083.

[22] Hayat, T., Ikram Ullah, A. Alsaedi, and M. Farooq. "MHD flow of Powell-Eyring nanofluid over a non-linear stretching sheet with variable thickness." *Results in Physics* 7 (2017): 189-196.DOI:https://doi.org/10.1016/j.rinp.2016.12.008.
[23] Ahmed, B., T. Hayat, Khursheed Muhammad, and A. Alsaedi. "MHD peristaltic activity of Powell-Eyring nanomaterial through porous space with slip effects." *Case Studies in Thermal Engineering* 45 (2023): 103001. DOI:https://doi.org/10.1016/j.csite.2023.103001.
[24] Ali, Qasim, Samia Riaz, and Aziz Ullah Awan. "Free convection MHD flow of viscous fluid by means of damped shear and thermal flux in a vertical circular tube." *Physica Scripta* 95, no. 9 (2020): 095212. DOI: 10.1088/1402-4896/abab39.
[25] Nisar, Zahid, Bilal Ahmed, Arsalan Aziz, Khursheed Muhammad, Hamiden Abd El-Wahed Khalifa, and Irshad Ahmad. "Mathematical modeling and analysis for radiative MHD peristaltic flow of Bingham nanofluid." *ZAMM-Journal of Applied Mathematics and Mechanics/Zeitschrift für Angewandte Mathematik und Mechanik* 104, no. 11 (2024): e202300840.DOI: https://doi.org/10.1002/zamm.202300840.
[26] Suzumura, Yoshikazu, and Kanji Ishino. "Effect of a Sinusoidal Magnetic Field on Superconductors in One-Dimensional Model." *Progress of Theoretical Physics* 67, no. 6 (1982): 1668-1674. DOI:https://doi.org/10.1143/PTP.67.1668
[27] Liao, Shijun. "On the homotopy analysis method for nonlinear problems." Applied mathematics and computation 147, no. 2 (2004): 499-513.DOI:https://doi.org/10.1016/S0096-3003(02)00790-7.
[28] Abbasbandy, S. "Homotopy analysis method for heat radiation equations." *International communications in heat and mass transfer* 34, no. 3 (2007): 380-387.DOI:https://doi.org/10.101 6/j.icheatmasstransfer.2006.12.001.
[29] Niu, Zhao, and Chun Wang. "A one-step optimal homotopy analysis method for nonlinear differential equations." *Communications in Nonlinear Science and Numerical Simulation* 15, no. 8 (2010): 2026-2036. DOI:https://doi.org/10.1016/j.cnsns.2009.08.014.
[30] Zubair, Tamour, Muhammad Usman, Umair Ali, and Syed Tauseef Mohyud-Din. "Homotopy analysis method for system of partial differential equations." *International Journal of Modern Engineering Sciences* 1, no. 2 (2012): 67-79.
[31] Asha, S. K., and Joonabi Beleri. "Peristaltic flow of Carreau nanofluid in presence of Joule heat effect in an inclined asymmetric channel by multi-step differential transformation method." *World Scientific News* 164 (2022): 44-63.
[32] Kotnurkar, Asha S., and Santosh Gowda. "Influence of magnetic field and activation energy on creeping flow of tri-hybrid nanofluid driven by peristaltic pumping in an asymmetric channel with synthetic cilia." *Discover Mechanical Engineering* 3, no. 1 (2024): 38. DOI:https://doi.org/10.1007 /s44245-024-00074-3.
[33] Kotnurkar, Asha S., and Sunitha, G. "Effect of joule heating and MHD on peristaltic blood flow of Eyring–Powell nanofluid in a non-uniform channel." *Journal of Taibah University for Science* 13, no. 1 (2019): 155-168. DOI:https://doi.org/10.1080/16583655.2018.1549530.
[34] Riaz, Arshad, R. Ellahi, and Sadiq M. Sait. "Role of hybrid nanoparticles in thermal performance of peristaltic flow of Eyring–Powell fluid model." *Journal of Thermal Analysis and Calorimetry* 143 (2021): 1021-1035. DOI:https://doi.org/10.1007/s10973-020-09872-9.
[35] Kotnurkar, Asha S., and Deepa C. Katagi. "Thermo-diffusion and diffusion-thermo effects on MHD third-grade nanofluid flow driven by peristaltic transport." *Arabian Journal for Science and Engineering* 45, no. 6 (2020): 4995-5008.DOI:https://doi.org/10.1007/s13369-020-04590-8.
[36] Jayavel, Prakash, Ravinder Jhorar, Dharmendra Tripathi, and Martin N. Azese. "Electroosmotic flow of pseudoplastic nanoliquids via peristaltic pumping." *Journal of the Brazilian Society of Mechanical Sciences and Engineering* 41, no. 2 (2019): 61. DOI: https://doi.org/10.1007/s40430-018-1555-0.